

Cite this: *Phys. Chem. Chem. Phys.*, 2012, **14**, 8711–8722

www.rsc.org/pccp

PAPER

Electronic structure, molecular electrostatic potential and spectral characteristics of pillar[6]arene hosts and their complexes with *n*-octyltriethylammonium ions

Swarada R. Peerannawar and Shridhar P. Gejji*

Received 18th October 2011, Accepted 28th March 2012

DOI: 10.1039/c2cp23280d

Electronic structure, charge distribution and ^1H NMR in pillar[6]arene (P6) conformers, their diisobutoxy derivatives and their host–guest complexes have been investigated by employing the density functional theory. It has been shown that a P6 conformer obtained by flipping of alternate hydroquinone units turns out to be of lowest energy, owing to the hydrogen bonded network at both rims of the host. As opposed to this, a conformer void of hydrogen bonding interactions has largely been destabilized. The O–H \cdots O interactions are analyzed using molecular electrostatic potential topography as a tool. Modification of a P6 host by substituting a diisobutoxy group at reactive phenols (DIBP6) renders rigid pillar-shape architecture to the host in which electron-rich regions are localized within the cavity and near portals. Complexation of *n*-octyltriethylammonium ions (*n*-OTEA) with P6 and DIBP6 reveals qualitatively different binding patterns. It has been shown that the conformer in which *n*-OTEA penetrates from the lower rim of the host and partially encapsulates within the P6 cavity turns out to be 1.4 kJ mol $^{-1}$ lower in energy than the complex showing complete guest encapsulation. Host–guest binding patterns, *viz.* encapsulation or portal interactions, can be distinguished from ^1H NMR chemical shifts. The shielding of ethyl and *n*-octyl chain protons in an *n*-OTEA \subset DIBP6 complex points to encapsulation of the guest which has been rationalized from natural bond orbital analyses. These inferences are in consonance with ^1H NMR experiments.

Introduction

Design and synthesis of new macrocyclic hosts with rigid architecture, conducive to stable complexes with organic, inorganic cations or neutral molecules, has been the focus of attention in the recent years. In view of this, cyclodextrin, cucurbituril and calixarene macrocycles and their derivatives have been explored in a variety of applications.^{1–23} Very recently a family of novel hosts possessing *para*-bridged cyclo-oligomers of phenol endowed with pillar-like structure has been reported.²⁴ These new pillar[*n*]arenes are comprised of repeating hydroquinone units condensed through a methylene bridge at the 1,4 position (*cf.* Fig. 1) where '*n*' denotes the number of units. Unlike vase-shaped calix[*n*]arene analogs, pillar[*n*]arene hosts are rendered with a cylindrical framework, which provides easy access for guest molecules for formation of host–guest complexes. Ogoshi and co-workers synthesised pillar[5]arene (P5) by condensation of 1,4-dimethoxybenzene (DMB) with *para* formaldehyde and appropriate Lewis acid catalyst followed by demethylation in the presence of

boron tribromide.²⁴ The hydroquinone pentamer exhibits excellent solubility as well as selective binding affinity toward cationic guests. Ogoshi and coworkers^{25–29} analyzed conformational features of P5 from ^1H NMR experiments. These authors pointed out that rotation behaviour of a phenolic unit in P5 depends on temperature, type of solvent, encapsulation of the guest and is controlled by introducing a bulky substituent.³⁰ The host further can be modified by substitution of alkyl, amine or aromatic groups at the reactive phenolic units on either or both rims of the host. Consequent to this functionality, asymmetric synthesis and formation of host–guest complexes of pillar[*n*]arene macrocycles have been analyzed. Li *et al.*³¹ carried out ^1H NMR, ESI mass and UV-vis absorption spectroscopy experiments on inclusion behaviour of P5 hosts with paraquat and bis(pyridinium) derivatives as guest molecules. Different binding modes and varying stoichiometry were systematically analyzed, which provided reference to understand molecular recognition and assemblies in supramolecular hosts. Ogoshi *et al.*^{32,33} investigated formation of polyrotaxane and polypsuedorotaxane with cationic viologen polymers. It is gratifying to note that shuttling behaviour of the P5 affects electron transfer from a donor (host) to an acceptor (cationic guest) and P5 based polyrotaxanes further

Department of Chemistry, University of Pune, Pune 411 007, India.
E-mail: spgejji@chem.unipune.ac.in; Fax: +91-20-225691728

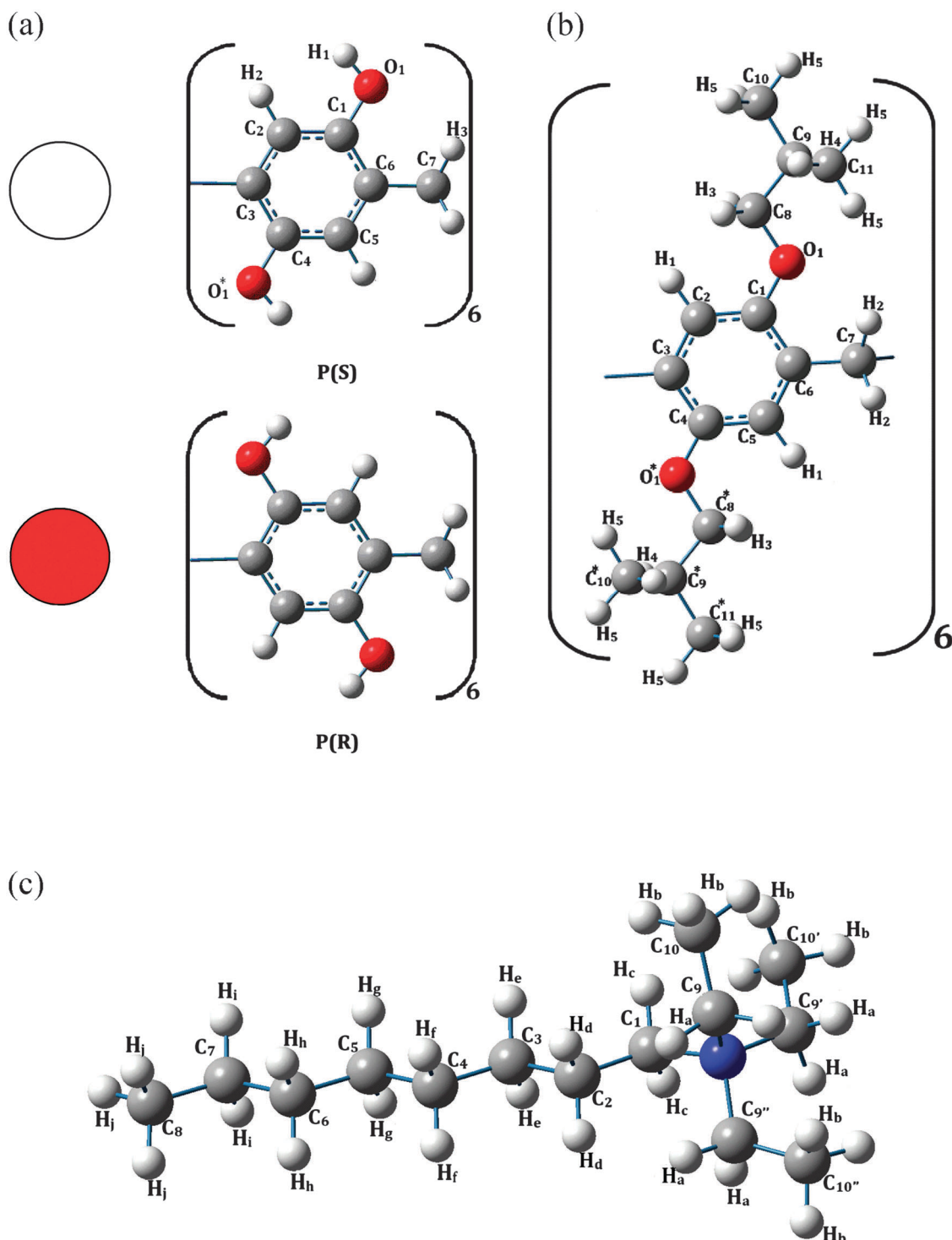


Fig. 1 (a) P(S) and P(R) enantiomers of P6 monomer, (b) monomer in DIBP6, (c) *n*-OTEA guest.

have potential applications in topological gels and multivalent scaffolds.³⁴ Moreover, decaamine-substituted P5 hosts with their remarkable binding affinity toward linear diacids have led to formation of stable pseudo[2]rotaxanes.³⁵ It has also been demonstrated that chiral substitution of P5 brings about rapid transformation and thus yields excess of either form of diastereomers.³⁶ The inter-conversion between *P*(S) and *P*(R) enantiomers of P5 or modified P5 hosts, in particular response to external stimuli such

as temperature, solvent or achiral guest addition, is crucial for chiral switching which can further be explored in chiral sensors, data storage and optical devices. It should further be remarked here that self-assembly of P5 provides guidelines to devise a new strategy for constructing organic nanotubes. The tubular structure underlying these nanotubes serves as a model for proton transport in biological channels.³⁷ Structural features of substituted P5 hosts have widely been investigated in recent years.^{38–47}

A yet another simple preparation of P5 and its higher homologue reported by Cao *et al.*⁴⁸ revealed that the use of a catalyst or different starting material improves the yield of these novel hosts. Pursuant to this, diisobutoxy substituted pillar[n]arenes ($n = 5, 6$) have been characterized from X-ray crystal structure data and ^1H NMR experiments. Selectivity of pillararenes toward binding of *n*-octyltriethylammonium (*n*-OTEA) ions has further been investigated.⁴⁹ A facile route to synthesise pillar[6]arenes (P6) with enhanced yield has been developed by Meier and co-workers.⁵⁰ Moreover, *n*-cetyl-trimethyl ammonium bromide encapsulated pillar[n]arenes further demonstrated selective binding of these hosts. The density functional calculations on structurally similar pillar[n]quinones have recently been carried out by Lao and Yu. Increasing the inner cavity along pillar[n]quinones series brings about large charge transfer resulting from electronic distribution in frontier molecular orbitals and dipole moments in ground and excited triplet states.⁵¹

Despite experimental investigations outlined above, almost no endeavour, be it *ab initio* or be it within DFT, has been made toward understanding of host–guest binding in pillar[n]arene hosts. Gejji *et al.*^{52–57} have shown that topography of scalar fields such as molecular electrostatic potential or molecular electron density from quantum chemical or density functional calculations has proven useful to understand interactions of cyclodextrin or cucurbituril hosts. The present work focuses on interactions between P6 hosts and *n*-octyltriethylammonium ions (*n*-OTEA) and how underlying cooperativity^{58,59} in a hydrogen bonding network affects the energies and chemical shifts in ^1H NMR spectra on complexation. The following questions have been addressed. How flipping of one or more hydroquinone monomer(s) of P6 influences energetics in different conformers? How substitution of a diisobutoxy functionality at the reactive hydroxyl group of P6 leads to different host–guest binding patterns? How binding of P6 and diisobutoxy pillar[6]arene (DIBP6) with cationic *n*-OTEA can be rationalized? How such host–guest interactions affect ^1H NMR chemical shifts in P6 or DIBP6? The computational method is outlined below.

Computational method

Geometry optimization within the framework of density functional theory, incorporating Becke's three-parameter⁶⁰ exchange coupled with Lee, Yang, and Parr's correlation functional (B3LYP),⁶¹ was performed on P6 conformers, DIBP6, *n*-OTEA guest and their complexes by employing Gaussian09 program.⁶² The internally stored 6-31G(d,p) basis set was used. Molecular electrostatic potential (MESP) analysis was carried out in P6 and DIBP6 hosts to identify electron-rich regions. The MESP $V(\mathbf{r})$ at a spatial point \mathbf{r} is given by

$$V(\mathbf{r}) = \sum_A^N \frac{Z_A}{|\mathbf{r} - \mathbf{R}_A|} - \int \frac{\rho(\mathbf{r}') d^3 r'}{|\mathbf{r} - \mathbf{r}'|}, \quad (1)$$

where N is the total number of nuclei in the molecule, Z_A defines the charge of the nucleus located at \mathbf{R}_A and $\rho(\mathbf{r})$ is the electron density at location \mathbf{r} . The two terms in the above equation refer to the bare nuclear potential and the electronic

contributions, respectively. Regions conducive to the electrophilic interactions are governed by substantial negative values of MESP.^{63,64} The topography in MESP was then mapped by examining eigenvalues of the Hessian matrix at a point where the gradient of $V(\mathbf{r})$ vanishes,^{65,66} and the critical points (CPs) were thereby located using the program code written in our laboratory. The CPs are characterized in terms of an ordered pair (R, σ) , where R denotes the rank (non-zero eigenvalues) and σ denotes the signature (the sum of algebraic signs of the eigenvalues) of the Hessian matrix, respectively, and fall into three categories: (3, +3), (3, +1) and (3, -1). The (3, +3) CP corresponds to the local minima, which represents potential binding sites for electrophilic interactions, whereas (3, +1) and (3, -1) refer to the saddle points. A locally written program UNIVIS-2000 was used for visualization of isosurfaces.⁶⁷ Bader *et al.*^{68–70} suggested that hydrogen bond interactions can be inferred from the presence of a bond critical point (bcp) in molecular electron density (MED) topography within the framework of Quantum Theory of Atoms in Molecules (QTAIM). It was suggested that the strength of a bond can be gauged from electron density at the bcp (ρ_{bcp}) in MED topography. In the present work we located bcps in different P6 conformers by employing a locally written program in our laboratory.⁷¹ To gain insights into complexation of (P6) and (DIBP6) hosts with the *n*-OTEA guest, different initial geometries, including the triethylammonium group of *n*-OTEA within the host cavity, secondly the triethylammonium group partly within the cavity and the *n*-octyl part protruding outside and finally *n*-OTEA excluding the host cavity and facilitating interactions with one of the host portals, were considered. The interaction energies were calculated by subtracting the sum of electronic energies of the P6 and DIBP6 hosts and the *n*-OTEA guest from that of their complex. Subsequently, natural bond orbital (NBO) analyses have also been carried out.⁷² ^1H NMR chemical shifts (δ_{H}) were obtained by subtracting the nuclear magnetic shielding tensors of protons in hosts, guests and complex from those of the tetramethylsilane (reference) using the gauge-independent atomic orbital (GIAO)⁷³ method. The effect of solvent (chloroform) on ^1H NMR chemical shifts was modelled by self-consistent reaction field (SCRF)⁷⁴ calculations by incorporating the polarizable continuum model (PCM).

Results and discussion

Optimized geometries of P6 and DIBP6 host monomers as well as the cationic *n*-OTEA guest are shown in Fig. 1. P6 is a cyclic hexamer of hydroquinone possessing a uniform cavity with six hydroxyl groups each at the top as well as the lower rim of the host. Fig. 1(a) shows two enantiomers of P6. Different conformers of P6 were derived by either successive or alternate rotation of phenolic units around the methylene bridge axis. A flipped monomer is schematically shown in red in Fig. 1. Gejji and coworkers⁷⁵ recently analyzed electronic structure and ^1H NMR of a Cl^- encapsulated bambus[6]juril host, incorporating X3LYP, B3LYP, PBE0, BMK and M06 exchange–correlation functionals in the regime of density functional theory. The structure and NMR chemical shifts derived from B3LYP (or X3LYP) theory in host–guest

complexes were found to agree better with experiments. We therefore employ B3LYP/6-31G(d,p) calculations to derive insights into host–guest interactions between P6 or DIBP6 hosts and *n*-OTEA.

Optimized geometries of these conformers from B3LYP calculations are shown in Fig. 2. The intra-molecular hydrogen bonding network herein is depicted by broken lines. These conformers are labelled ‘A1’, ‘A2’ to ‘A6’. Conformer ‘A4’, ‘A3’ and ‘A5’ were obtained by rotation of one, two and three adjacent monomers, respectively. The ‘A3’ and ‘A5’ conformers engender distortion of the host cavity due to successive flipping while conformer ‘A4’ emerges with a uniform cavity. On the other hand, alternate rotation of two and three monomers yields ‘A2’ and ‘A1’ conformers. The ‘A1’ to ‘A5’ conformers possess different number of O–H···O’ interactions; where prime denotes oxygen from an adjacent hydroquinone unit. Thus ‘A4’, ‘A3’ and ‘A5’ conformers possess two O–H···O’ interactions. The conformer ‘A2’ possesses four O–H···O’ interactions whereas the ‘A1’ conformer comprises six O–H···O’ interactions (three from each rim). Conformer ‘A6’ refers to an enantiomer void of intra-molecular hydrogen bonding. In Table 1, the hydrogen bond

distances are reported along with the corresponding ρ_{bcp} values from QTAIM theory. It should be remarked here that the strength of the bond can be gauged from ρ_{bcp} values in MED topography.^{66–68} As may be noticed, ρ_{bcp} values of O–H···O bonds in ‘A1’ (and ‘A2’ and ‘A4’ conformers as well) turn out to be 0.031 au, compared to 0.023 au in the ‘A5’ conformer. It may thus be conjectured that stabilization of the ‘A1’ conformer (*cf.* Fig. 2) stems from the interplay between the number and strength of O–H···O’ interactions. In other words, alternate rotation of phenol units stabilizes P6 conformers. Accordingly energies (in kJ mol^{−1}) of different P5 conformers relative to its lowest energy ‘A1’ conformer turn out to be: ‘A2’ (21.4) < ‘A3’ (41.3) < ‘A4’ (45.5) < ‘A5’ (61.9) < ‘A6’ (72.4).

As pointed out in the Introduction, substitution at hydroxyl portals renders rigid structure and enhances affinity towards the guest. Thus P6 modified by substituting a diisobutoxy group at reactive phenolic unit(s) yields DIBP6; a monomer of which has been shown schematically in Fig. 1(b). Introducing a bulky substituent at the upper as well as lower rims sterically hinders conformation freedom and yields either form of enantiomer in DIBP6. Han *et al.*⁴⁹ elucidated X-ray crystal

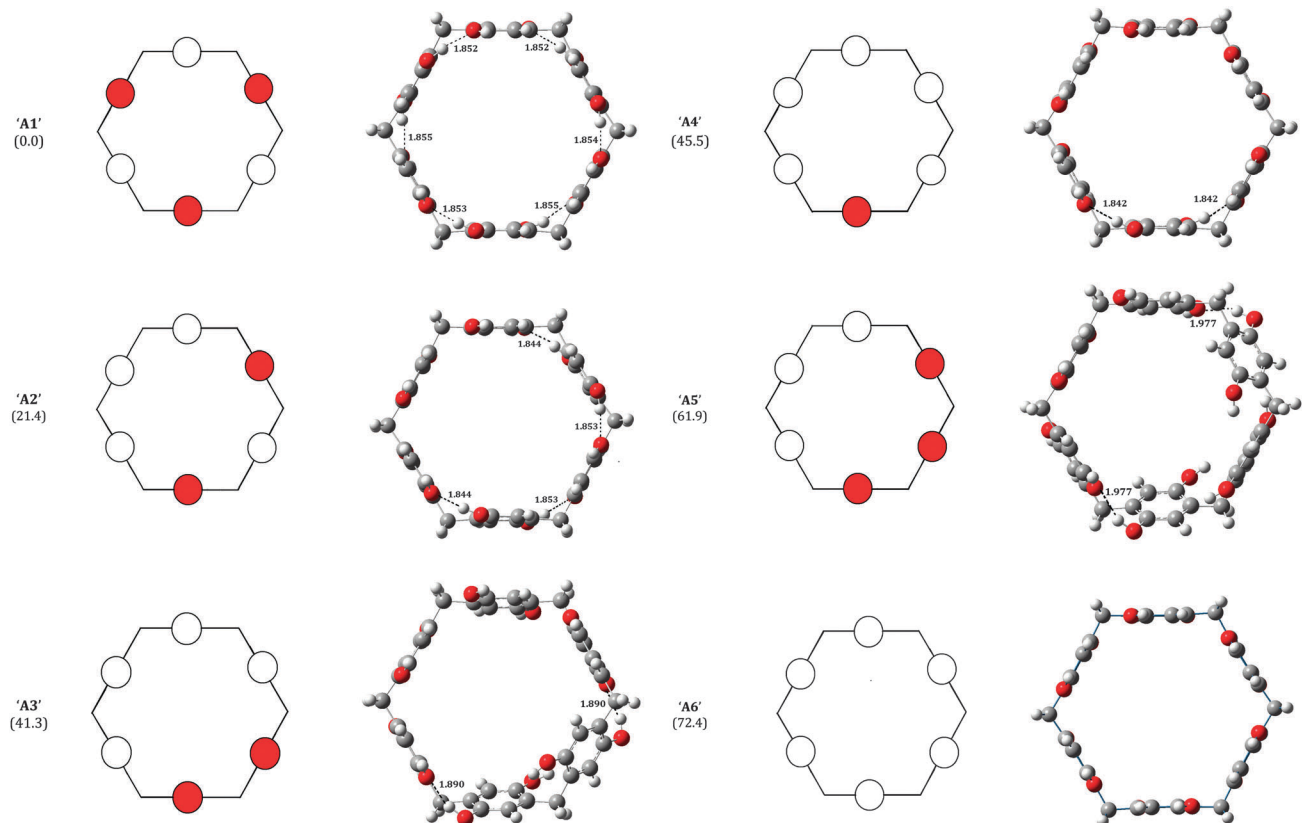


Fig. 2 B3LYP/6-31G(d,p) optimized P6 conformers (relative stabilization energies in kJ mol^{−1} given in parentheses).

Table 1 Intra-molecular O–H···O’ distances (in Å) in P6 conformers

	‘A1’	‘A2’	‘A3’	‘A4’	‘A5’
O ₁ –H···O’ _(top)	1.854(0.031)	1.844(0.031) 1.853(0.030)	1.890(0.028)	1.842(0.031)	1.977(0.023)
O ₂ –H···O’ _(bottom)	1.855(0.031)	1.844(0.031) 1.853(0.030)	1.890(0.028)	1.842(0.031)	1.977(0.023)

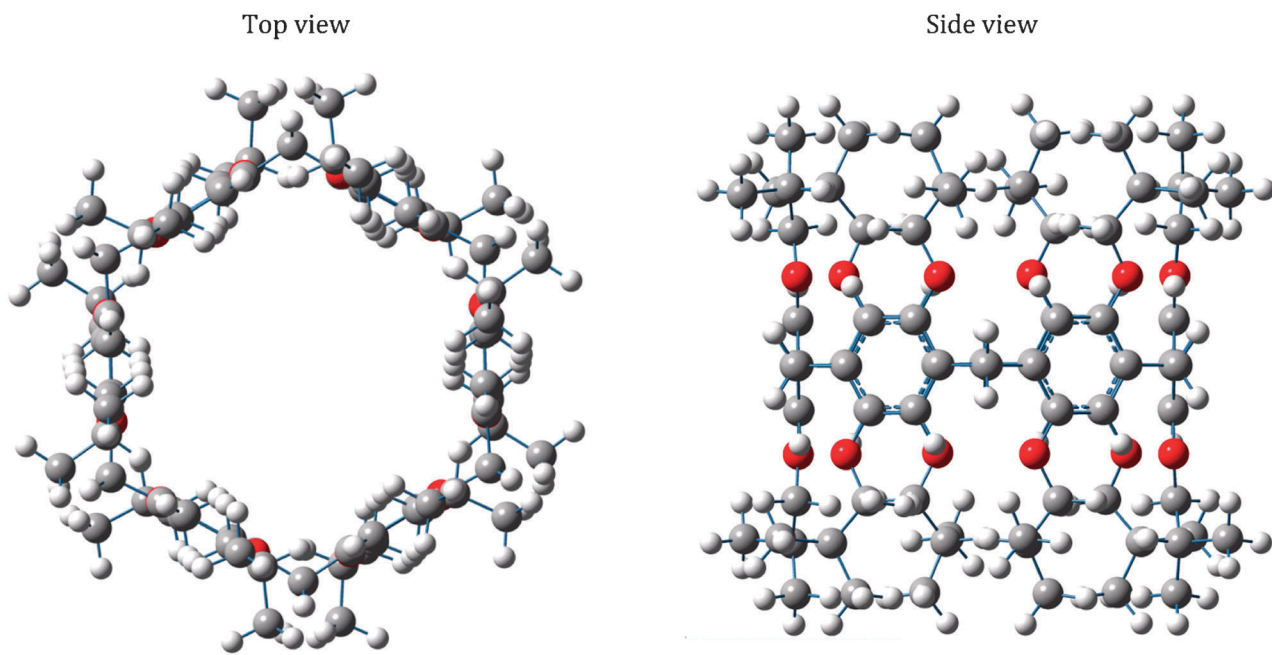


Fig. 3 B3LYP/6-31G(d,p) optimized DIBP6 host (top and side views).

structure of DIBP6 in a mixture of dichloromethane and acetonitrile which revealed trapping of solvent molecules in the host cavity. Theoretical calculations refer to an isolated molecule free from any intermolecular interactions. A direct comparison of DIBP6 from the present theory with crystal structure data is thus far from straightforward. Optimized geometry of a DIBP6 host (both top and side views) has been displayed in Fig. 3.

Selected geometrical parameters of lowest energy P6 and DIBP6 hosts are discussed below. The average bond distances and bond angles are given in Table 2. The –OH bond distances in hydrogen bonding (0.973 Å) are longer than those of non-participating hydroxyl groups (0.966 Å); concomitant shortening of aromatic C–H bonds (1.086 Å) was observed in the flipped monomer. The adjacent hydroxyl oxygens (O–O) in the ‘A1’ conformer get closer (2.823 Å) compared to DIBP6 in which they exhibit a separation of 5.231 Å. It may as well be

noticed that radially opposite hydroxyl oxygens from the upper rim (or the lower rim) are separated by 10.077 Å in P6 compared to those of 10.414 Å in DIBP6. *Para*-substituted hydroquinone oxygens ($O_1 - O_1^*$) are ~5.5 Å apart in both the hosts. The hydrogen bonded interactions in a P6 host reveal closure of $\angle C_1 - O_1 - H_1$ to 109.6°. On the other hand, opening of $\angle C_1 - O_1 - C_8$ to 118.5° can be observed for DIBP6.

X-ray crystal structure data on P5 point to a structure in which alternate rotation of two hydroquinone units engendering intra- as well as inter-molecular hydrogen bonded (with solvent) interactions has been noticed. It has been observed that flipping of monomers brings the hydroxyl oxygens closer. Moreover, the shortening of aromatic C–H bonds in the flipped monomer has been noticed. Furthermore, the –OH bond lengths in hydrogen bonded interactions are longer. These observations are parallel to the conclusions drawn from the present calculations as discussed earlier.

Table 2 Selected bond distances (in Angstrom) and bond angles (in degrees) in P6, DIBP6 hosts, *n*-OTEA guest and their complexes

	P6	DIBP6	<i>n</i> -OTEA	<i>n</i> -OTEA ⊂ P6	<i>n</i> -OTEA ⊂ DIBP6
$O_1 - O_1$	2.823	5.231		2.809	5.468
$O_1 - O_1^*$	5.541	5.554		5.539	5.554
$C_1 - O_1$	1.385(1.369 ^a)	1.379		1.386(1.376 ^a)	1.381
$O_1 - H_1$	0.966(0.973 ^a)			0.966(0.974 ^a)	
$C_2 - H_2$	1.088(1.086 ^a)			1.089(1.086 ^a)	
$O_1 - C_8$		1.422			1.428
$C_6 - C_7 - C_3$	115.5	115.3		115.1	115.3
$C_1 - O_1 - H_1$	110.3(109.6 ^a)			110.4(112.3 ^a)	
$C_1 - O_1 - C_8$	118.5				114.3
$O_1 - C_8 - C_9$	108.9				109.1
$C_2 - C_1 - O_1 - H_1$	7.3(156.4 ^a)			8.1(168.9 ^a)	
$C_2 - C_1 - O_1 - C_8$		2.6			28.1
$C_1 - O_1 - C_8 - C_9$		176.0			169.3
$N - C_9$			1.538	1.533	1.533
$N - C_9 - C_{10}$			117.3	116.5	117.1
$N - C_1 - C_2 - C_3$			177.3	165.0	171.3

^a –OH in hydrogen bonding (flipped monomer).

Molecular electrostatic potential in P6 conformers displayed in Fig. 4 reveals electron-rich regions in the molecular system. An isosurface of $V = -100.8 \text{ kJ mol}^{-1}$ in P6 conformers is shown. It is readily discernible that the negative potential has largely been localized near the flipped hydroquinone unit of the host. Thus hydroxyl oxygens participating in hydrogen bonding exhibit large electron-rich regions. MESP minima near hydroxyl oxygens are denoted “*x*” (blue) and those inside the cavity are referred to as “*y*” (red). Likewise, minima located outside the cavity are designated “*z*” (green). A pair

of MESP minima (*y*) was identified for each aromatic ring of a P6 host when it does not participate in hydrogen bonding. The MESP minima within the aromatic cavity disappear upon flipping of the hydroquinone monomer as a result of an extended hydrogen bonding network. It may therefore be conjectured that the number of MESP minima within the host cavity provides measure of stability in P6 conformers. Accordingly six and twelve, respectively, MESP minima were located in the lowest energy ‘A1’ and largely destabilized ‘A6’ conformers. A top view of the array of MESP CPs in ‘A1’ and

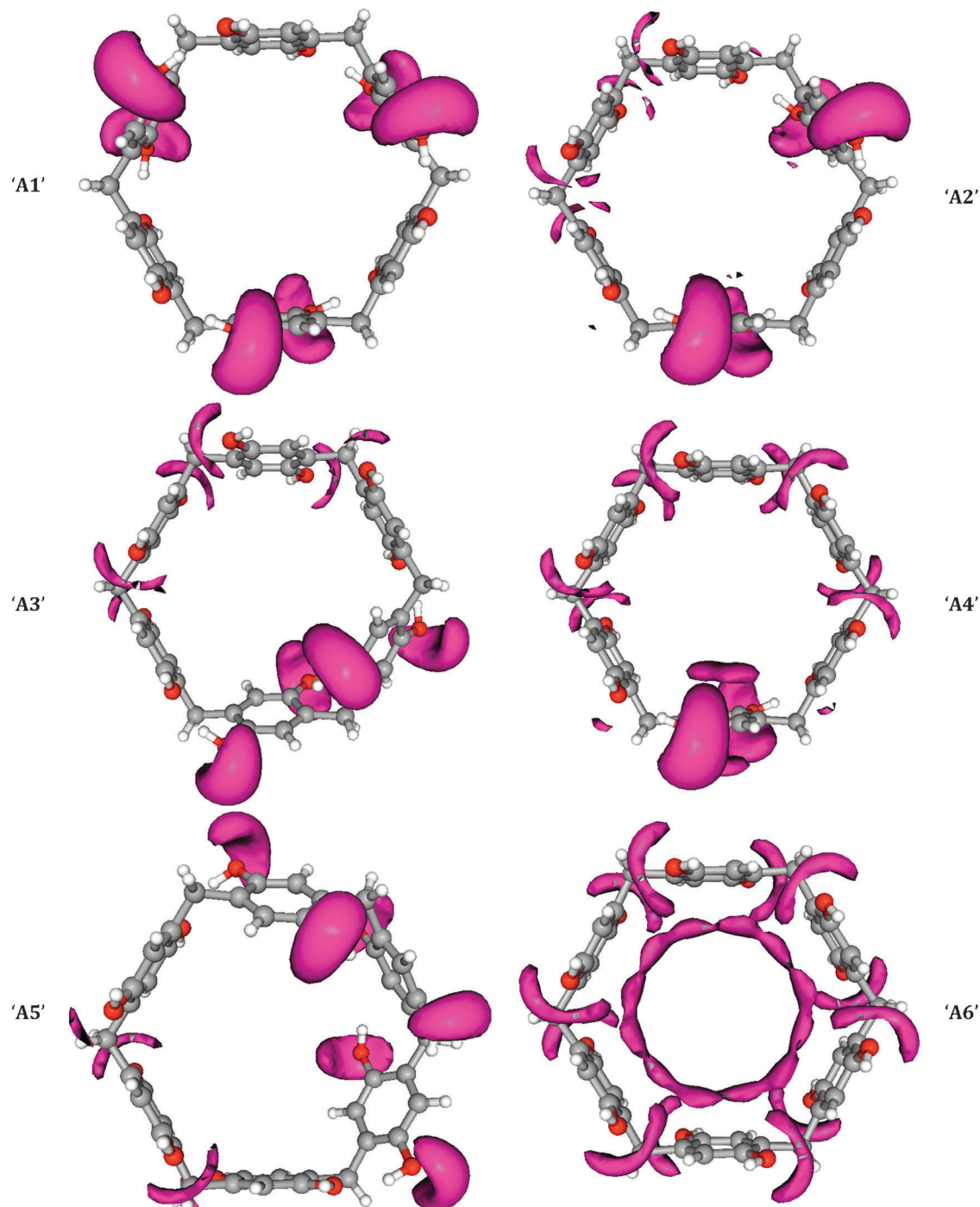


Fig. 4 MESP isosurface ($V = -100.8 \text{ kJ mol}^{-1}$) in P6 conformers.

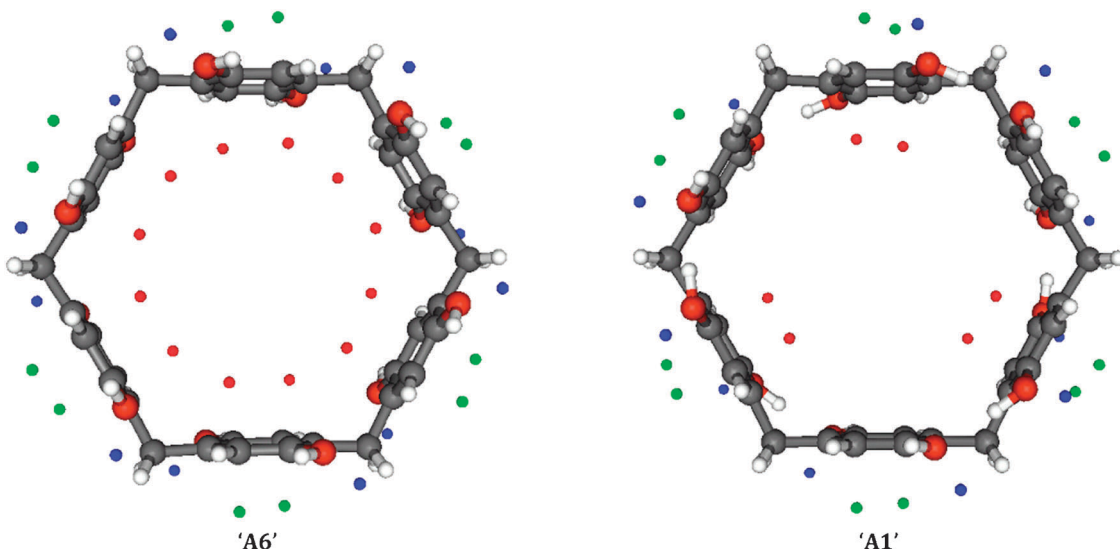


Fig. 5 Top view of the array of MESP CPs in 'A1' (lowest energy) and 'A6' (void of hydrogen bonding) conformers.

'A6' conformers is depicted in Fig. 5. The MESP isosurface ($V = -100.8 \text{ kJ mol}^{-1}$) in DIBP6 displayed in Fig. 6 reveals electron-rich regions near oxygen laced portals ($V = -138.6 \text{ kJ mol}^{-1}$) as well as within the host cavity ($V = -119.4 \text{ kJ mol}^{-1}$). Thus relatively large electron-rich character of the DIBP6 host cavity may favour encapsulation of *n*-OTEA over a P6 host. MESP minima for P6 and DIBP6 are reported in Table 3.

The *n*-OTEA guest with a cationic triethylammonium group and a longer *n*-octyl chain (*cf.* Fig. 1(c)) exhibits different modes of binding with P6 and modified DIBP6 hosts. Optimized geometries of *n*-OTEA \subset P6 complexes are depicted in Fig. 7(a) along with relative stabilization energy and binding energy (in kJ mol^{-1}) given in parentheses. The partially encapsulated guest interacts laterally with the lower portal and conducive inclusion of one ethyl group yields the lowest

Table 3 MESP minima in kJ mol^{-1} ('x' near hydroxyl/diisobutoxy oxygens whereas 'y' and 'z' for aromatic ring within and outside the cavity) in P6 and DIBP6 hosts

	'A1'	'A2'	'A3'	'A4'	'A5'	'A6'	DIBP6
'x'	-198.7 ^a -88.2	-208.8 ^a -114.8	-194.2 ^a -119.3	-218.9 ^a -135.2	-177.5 ^a -126.8	-152.2	-138.6
'y'	-86.1 -75.4	-98.9 ^a -75.4	-79.2 ^a -75.9	-111.5 ^a -90.0	-44.0 ^a -61.9	-103.9	-119.4
'z'	-86.6 ^a -28.3	-97.5 ^a -49.3	-75.0 ^a -59.2	-108.1 ^a -65.3	-77.5 ^a -43.2	-80.8	-91.5

^a Flipped monomer.

energy complex ('C1'). The energy lowering of 'C1' has partly been attributed to C–H \cdots O interactions from one of the ethyl protons. A complete encapsulation of *n*-OTEA yields conformer 'C2' which is marginally (1.4 kJ mol^{-1}) higher in energy than

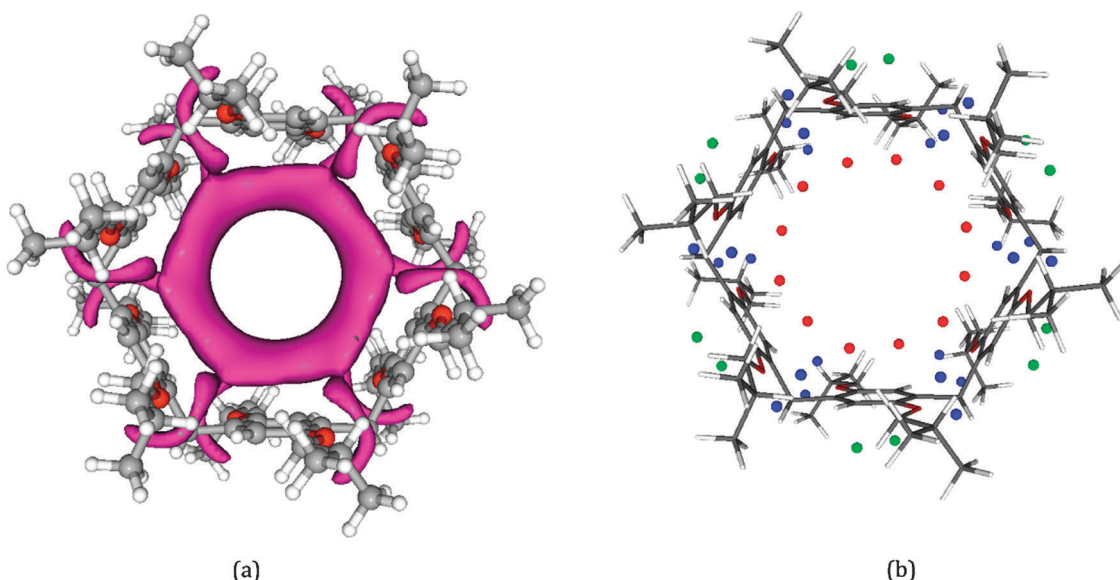


Fig. 6 (a) MESP isosurface ($V = -100.8 \text{ kJ mol}^{-1}$) in DIBP6 along with (b) array of CPs.

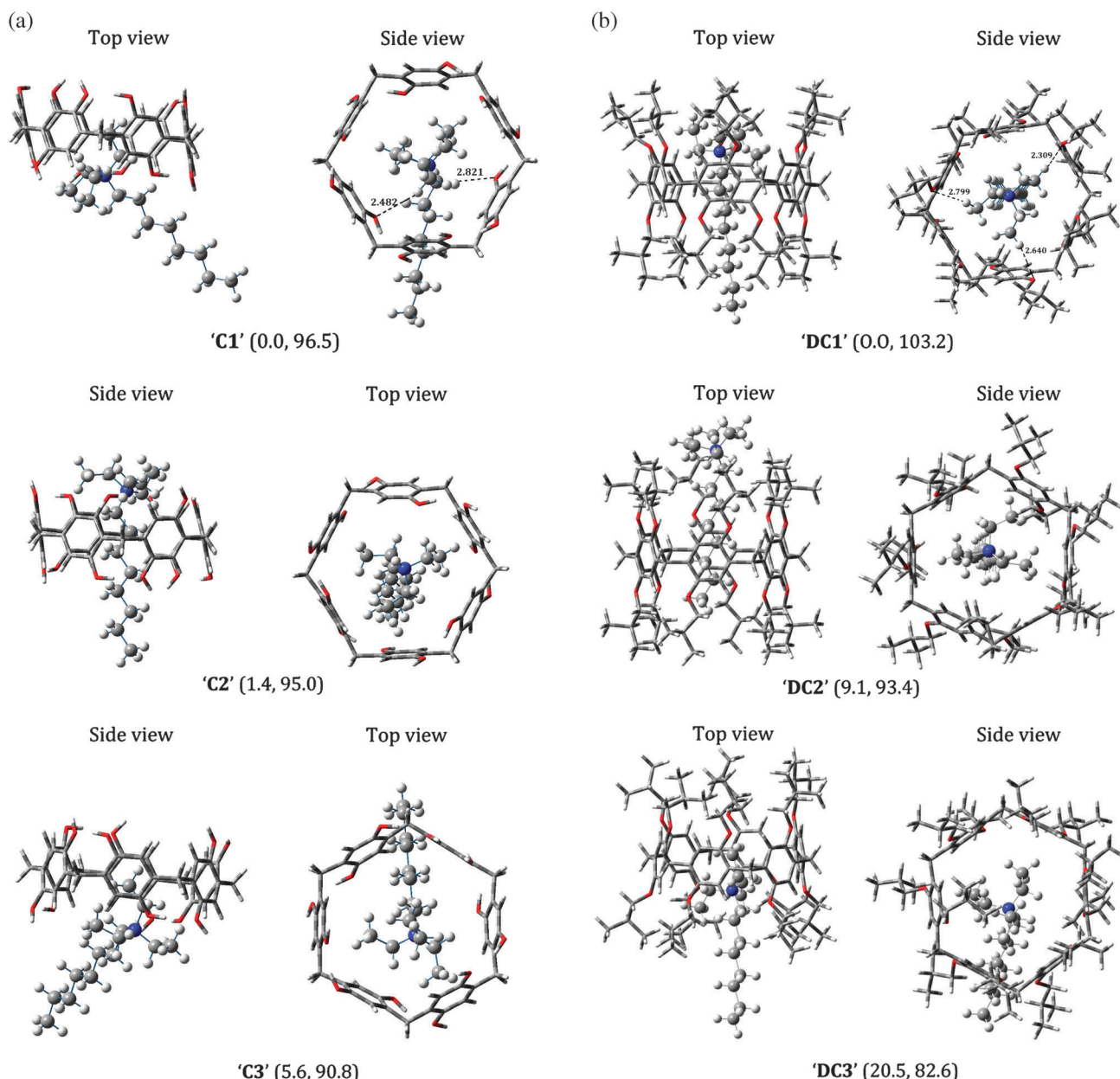


Fig. 7 B3LYP/6-31G(d,p) geometries: (a) *n*-OTEA \subset P6 and (b) *n*-OTEA \subset DIBP6 (both relative stabilization and interaction energies, in kJ mol $^{-1}$, given in parentheses).

its lowest energy structure. The conformer with the guest excluding the host cavity converged to structure 'C3' where interactions from the host portal can be noticed. Further a cationic moiety directing away from the host portal led to destabilization of 5.6 kJ mol $^{-1}$ over its lowest energy conformer.

The *n*-OTEA \subset DIBP6 complexes depicted in Fig. 7(b) converge to three distinct conformers. Here the lowest energy conformer with complete inclusion of the *n*-OTEA guest within the host cavity ('DC1') possesses C–H \cdots O interactions between the ethyl substituent and portal oxygens of the host. On the other hand, partial encapsulation of the guest on optimization converged to inclusion complex 'DC2' void of attractive hydrogen bonded interactions from the portal and hence destabilized by 9.1 kJ mol $^{-1}$ relative to the 'DC1' complex.

The conformer 'DC3' was predicted to be 20.5 kJ mol $^{-1}$ higher in energy where the triethylammonium group interacts laterally with the lower portal of the host and the *n*-octyl chain directing away from the cavity. The interaction energy of *n*-OTEA with DIBP6 was 103.2 kJ mol $^{-1}$ compared to 96.5 kJ mol $^{-1}$ in the case of the parent P6 host. These conclusions agree with those based on MESP investigations.

Selected geometrical parameters in *n*-OTEA \subset P6 and *n*-OTEA \subset DIBP6 complexes are compared with those in individual host and guest (*cf.* Table 2). Geometrical parameters in the *n*-OTEA \subset P6 complex are reported for the lower portal of the host that interacts with *n*-OTEA. Here adjacent oxygens (O₁–O₂) are separated by 2.809 Å compared to 2.823 Å in an isolated P6 host. The radially opposite hydroxyl oxygens

get closer (9.523 \AA) on partial encapsulation of *n*-OTEA. Bond angles are insensitive to complexation except for $\angle C_1-O_1-H_1$ participating in intra-molecular hydrogen bonding, which

deviates by 3° . Encapsulation of *n*-OTEA within DIBP6 results in expansion of the host cavity and larger separation of radially opposite monomers (11.195 \AA), which is also

Table 4 Electron density (in au) in O–H, C–O and C–H σ^* natural orbitals, Bond distances (r in \AA) in isolated hosts, *n*-OTEA guest and their complexes

	P6		DIBP6		<i>n</i> -OTEA		<i>n</i> -OTEA \subset P6		<i>n</i> -OTEA \subset DIBP6	
	σ^*	r	σ^*	R	σ^*	R	σ^*	r	σ^*	r
O–H ^c	0.0375	0.973					0.0352 ^a	0.974 ^a		
O–H	0.0077	0.966							0.0287	1.392
C–O			0.0284	1.379					0.0285	1.381
C–H ^a					0.0112	1.091	0.0193	1.093		
C–H ^b					0.0110	1.090	0.0135	1.091		
C–H ^b					0.0113	1.092			0.0147	1.094
C–H ^b					0.0110	1.090			0.0160	1.092

^a Methylene and ^b methyl protons of *n*-OTEA guest, ^c host protons participating in hydrogen bonding.

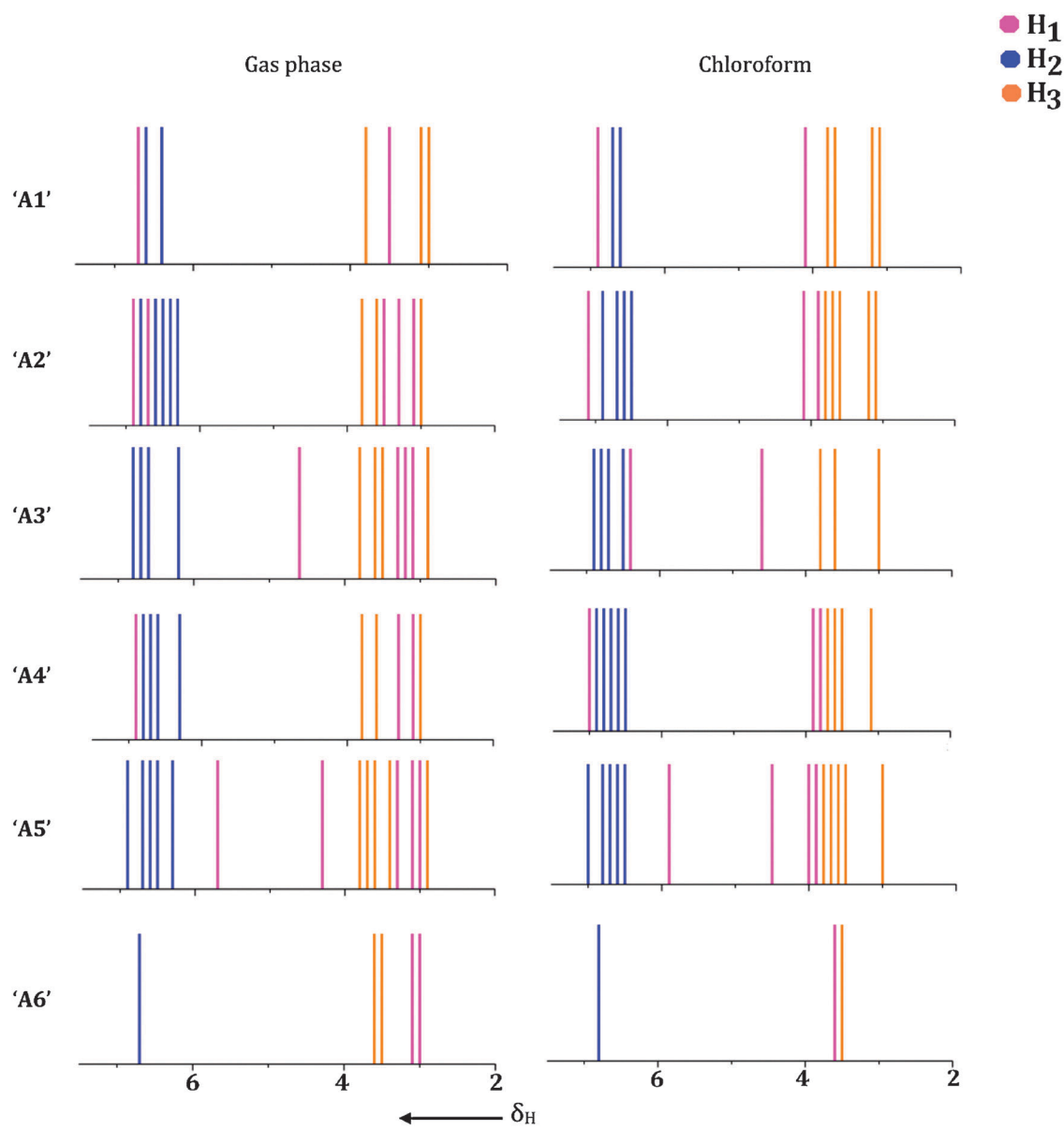


Fig. 8 ^1H NMR chemical shifts in P6 conformers.

Table 5 ^1H NMR chemical shifts for P6 conformers

	'A1'		'A2'		'A3'		'A4'		'A5'		'A6'	
	Gas	CHCl ₃	Gas	CHCl ₃								
H ₁	6.7 ^a 3.5	6.9 ^a 4.1	6.8 ^a 3.3	6.0 ^a 3.8	6.2 ^a 3.4	5.5 ^a 3.7	6.9 ^a 3.2	7.0 ^a 3.7	5.7 ^a 3.5	4.8 ^a 3.7	3.0	3.6
H ₂	6.5	6.6	6.5	6.7	6.6	6.7	6.6	6.7	6.6	6.7	6.7	6.8
H ₃	3.4	3.4	3.3	3.5	3.5	3.5	3.5	3.5	3.5	3.5	3.3	3.5

^a For proton participating in hydrogen bonding.

evident from separation of two adjacent oxygens (5.468 Å). Furthermore, N–C₉ bonds in *n*-OTEA are shortened in *n*-OTEA \subset P6 and *n*-OTEA \subset DIBP6 complexes. Closure of $\angle \text{C}_1\text{O}_1\text{C}_8$ from 118° in an isolated host to 114° was noticed in the DIBP6 complex. The dipole moments of close lying 'C1' and 'C2' conformers of the *n*-OTEA \subset P6 complex turn out to be 4.23 D and 7.60 D, respectively. Complete encapsulation of *n*-OTEA within the host cavity renders large dipole moment compared to those in 'C2' and 'DC1' (5.11 D) conformers of P6 and DIBP6 complexes.

To understand the bond strength variation in P6 and DIBP6 hosts on complexation with *n*-OTEA we utilize NBO analysis. Accordingly, the electron density of –OH and C–O antibonding orbitals (σ^*) in P6 and DIBP6 as well as C–H bonds of the *n*-OTEA guest are compared with those in free hosts and guest in Table 4. It may be noticed that the –OH participating in hydrogen bonding reveals increased electron density (0.037 au) in its antibonding natural orbital (σ^*) compared to that from non-participating ones (0.007 au) and consequently engenders downshifted signals in the ^1H NMR spectra. The weakening of C–H bonds from methylene of *n*-OTEA participating in hydrogen bonded interactions with P6 is evident from larger electron density in the C–H* natural (antibonding) orbital (by 0.008 au). Likewise, NMR signals of C–H protons in the guest reveal weakening of the corresponding bonds in the guest.

In the following, we discuss ^1H NMR chemical shifts of P6 and DIBP6 hosts, *n*-OTEA guest and their inclusion complexes. How successive or alternated rotation of a phenol unit in P6 affects ^1H NMR chemical shifts has been depicted in Fig. 8. A P6 host possesses three non-equivalent protons. The δ_{H} values of hydroxyl protons (H₁) involved in hydrogen bonding are distinctly downshifted (by ~6.7 ppm) whereas those of non-participating protons appear near 3.5 ppm. Average chemical shifts in gas phase as well as in chloroform (solvent) are compared in Table 5. The simulation of ^1H NMR in chloroform via SCRF calculations led to deshielding of the corresponding protons. Aromatic protons (H₂) emerge with δ_{H} near 6.6 ppm. Likewise methylene bridge protons (H₃) correspond to the signal at δ_{H} 3.4 ppm. As may be noticed H₂ and H₃ protons are unchanged upon flipping of monomers. It may as well be remarked here that ^1H NMR measurements by Ogoshi *et al.*²⁴ have shown that the δ_{H} signal at 7.9 ppm for hydroxyl protons in pillar[5]arene arises due to the interplay of inter-molecular and intra-molecular non-covalent hydrogen bonding interactions. The δ_{H} values in a P5 host then follow the order H₁ (7.9 ppm) > H₂ (6.6 ppm) > H₃ (3.5 ppm). The ^1H NMR of P6 measurements have not yet been reported in the literature

Table 6 ^1H NMR chemical shifts in P6 and DIBP6 hosts and their complexes

P6	<i>n</i> -OTEA \subset P6				DIBP6				<i>n</i> -OTEA \subset DIBP6	
	'C1'		'C2'		'C1'		'C2'		'DC1'	
	Gas	CHCl ₃	Gas	CHCl ₃	Gas	CHCl ₃	Gas	CHCl ₃	Gas	CHCl ₃
H ₁	6.7 ^a 3.5	6.9 ^a 4.1	6.4 ^a 3.7	6.5 ^a 4.2	6.4 ^a 3.7	6.6 ^a 4.2	7.1	7.2	7.2	7.2
H ₂	6.5	6.6	6.5	6.6	6.5	6.7	3.8	3.8	3.9	3.9
H ₃	3.4	3.4	3.5	3.5	3.6	3.5	3.7	3.8	3.7	3.8
H ₄							2.4	2.4	2.3	2.4
H ₅							1.1	1.1	1.2	1.3

^a Proton participating in hydrogen bonding in P6.

Table 7 δ_{H} values in free *n*-OTEA guests and their complexes with P6 ('C1' and 'C2' conformers) and DIBP6 hosts

<i>n</i> -OTEA	<i>n</i> -OTEA \subset P6				<i>n</i> -OTEA \subset DIBP6			
	'C1'		'C2'		'C1'		'C2'	
	Gas	CHCl ₃	Gas	CHCl ₃	Gas	CHCl ₃	Gas	CHCl ₃
H _a	3.1	3.3	2.2	2.2	2.8	2.9	2.1	2.2
H _b	1.5	1.4	1.3	−0.7	1.2	1.3	0.5	0.6
							2.4 ^a	2.3 ^a
H _c	3.0	3.1	2.9	3.0	1.5	1.5	0.8	0.9
H _d	1.6	1.7	1.7	1.7	−0.5	−0.4	−0.4	−0.4
H _e	1.3	1.4	1.3	1.4	−0.6	−0.6	0.1	0.1
H _f	1.5	1.4	1.5	1.5	0.2	0.2	0.8	0.9
H _g	1.4	1.4	1.5	1.5	0.9	0.9	1.2	1.3
H _h	1.4	1.3	1.4	1.4	1.0	1.1	1.5	1.5
H _i	1.4	1.4	1.5	1.5	1.5	1.4	1.5	1.5
H _j	0.9	0.9	1.0	1.0	1.0	1.0	1.1	1.1

^a *n*-OTEA protons participating in hydrogen bonding.

and therefore a comparison of calculated chemical shifts in P6 with those of experiment is not possible. The present calculations have shown that protons from hydrogen bonding interaction reveal largest deshielding. A DIBP6 host possesses five non-equivalent protons H₁, H₂ to H₅. In Table 6 aromatic H₁ protons of DIBP6 display large deshielding (δ_{H} 7.1 ppm) compared to the corresponding H₂ proton in a P6 host. The methylene bridge protons (H₂) correspond to δ_{H} 3.8 ppm. The δ_{H} values from experiment⁴⁹ follow the trend: H₁ (7.9 ppm) > H₂ (3.8 ppm) > H₃ (3.5 ppm) > H₄ (1.9 ppm) > H₅ (0.9 ppm), which is in consonance with the present theory. Furthermore, δ_{H} signals due to H₁, H₄ and H₅ protons are deshielded and deviated by 0.5 ppm from those in observed spectra. ^1H NMR signals in DIBP6 are not influenced significantly on complexation as seen from δ_{H} values of an

individual host and its complexes in gas phase and in chloroform (solvent) given in Table 6.

NMR chemical shifts in unbound *n*-OTEA and its complexes with P6 and DIBP6 are reported in Table 7. The shielding of triethyl groups (H_a and H_b) was noticed in conformer ‘C1’ consequent to encapsulation from the lower rim of the host. The *n*-octyl protons directing outside the cavity are nearly insensitive to complexation. It should be remarked here that NMR signals of methylene protons on the terminal *n*-octyl chain serve as a probe to distinguish encapsulation or lateral interactions in host–guest binding. The δ_H values of the H_g proton in the ‘C1’ complex of *n*-OTEA \subset P6 (1.5 ppm) are unchanged, while encapsulation of the guest in the ‘C2’ conformer engenders shielding of the corresponding proton with $\delta_H = 0.9$ ppm. Likewise δ_H signals of triethyl as well as *n*-octyl protons support complete *n*-OTEA encapsulation of the DIBP6 complex. Furthermore, C–H \cdots O interactions from an ethylene proton (H_b) emerge with δ_H signals near 2.4 ppm. As pointed out earlier, the enhanced or depleted electron density near protons has been inferred from NBO analysis which further rationalizes deshielding (or shielding) from δ_H signals in ^1H NMR spectra. The solvent (chloroform) merely influences ^1H NMR shifts of guest protons and consequent spectra agree well with those observed in experiments.

Conclusions

Binding patterns of the *n*-OTEA guest with P6 and DIBP6 hosts have been systematically analyzed within the framework of density functional theory. Conformational analysis of P6 hosts has shown that the conformer comprising of alternate rotation of hydroquinone monomers is of lowest energy, which attributes to intra-molecular hydrogen bonding at both rims. MESP investigations further suggest that electron-rich regions are largely associated with flipped monomer(s). Diisobutoxy substitution at the reactive phenols of P6 engenders deeper minima near portal oxygens and within the cavity of DIBP6. Two distinct conformers of *n*-OTEA \subset P6 possessing lateral interaction with the host portal and encapsulation of the guest within the host cavity were characterized, which differ in energy merely by ~ 1.4 kJ mol $^{-1}$ and can be distinguished from terminal *n*-octyl chain proton signals in the ^1H NMR spectra. In the *n*-OTEA \subset DIBP6 complex the guest resides entirely within the DIBP6 cavity, facilitating hydrogen bonded interactions, which is accompanied by cavity expansion to accommodate a bulky cationic guest, as evident from shielding of guest protons. These inferences are supported by NBO analysis and experimental ^1H NMR as well.

Acknowledgements

S.P.G. is grateful to the University Grants Commission (UGC), New Delhi, India [Research Project F34-370/2008(SR)], and University of Pune for distributing the research grant under the potential excellence scheme.

References

- K. Uekama, *J. Inclusion Phenom. Macrocyclic Chem.*, 2002, **44**, 3.
- K. Takahashi, *Chem. Rev.*, 1998, **98**, 2013.
- K. Kano and H. Hasegawa, *J. Inclusion Phenom. Macrocyclic Chem.*, 2001, **41**, 41.
- H. J. Buschmann, D. Knittel and E. Schollmeyer, *J. Inclusion Phenom. Macrocyclic Chem.*, 2001, **40**, 169.
- S. Monti and S. Sortino, *Chem. Soc. Rev.*, 2002, **31**, 287.
- A. Harada, *Acc. Chem. Res.*, 2001, **34**, 456.
- Y. C. Guillaume and C. Guinchard, *J. Phys. Chem. B*, 1997, **101**, 8390.
- H. C. Kolb, M. G. Finn and K. B. Sharpless, *Angew. Chem., Int. Ed.*, 2001, **40**, 2004.
- D. Tuncel and J. H. G. Steinke, *Macromolecules*, 2004, **37**, 288.
- D. Tuncel and J. H. G. Steinke, *Chem. Commun.*, 2002, 496.
- P. Mukhopadhyay, A. Wu and L. Isaacs, *J. Org. Chem.*, 2004, **69**, 6157.
- C. A. Burnett, D. Witt, J. C. Fettinger and L. Isaacs, *J. Org. Chem.*, 2003, **68**, 6184.
- N. J. Wheate, A. I. Day, R. J. Blanch, A. P. Arnold, C. Cullinane and J. G. Collins, *Chem. Commun.*, 2004, 1424.
- R. Ludwig and N. T. K. Dzung, *Sensors*, 2002, **2**, 397.
- J.-S. Kim, W.-K. Lee, D.-Y. Ra, Y.-I. Lee, W.-K. Choi, K.-W. Lee and W.-Z. Won-Zin Oh, *Microchem. J.*, 1998, **59**, 464.
- V. Souchon, I. Leray and B. Valeur, *Chem. Commun.*, 2006, 4224.
- S. J. Harris and M. McManus, *Eur. Patent Appl. EP*, 1988, vol. 24, p. 279.
- P. K. Thallapally, G. O. Lloyd, J. L. Atwood and L. J. Barbour, *Angew. Chem.*, 2005, **44**, 3848.
- J. W. Steed, R. K. Juneja, R. S. Burkhalter and J. L. Atwood, *J. Chem. Soc., Chem. Commun.*, 1994, 2205.
- L. Baldini, C. Barcchini, R. Cacciapaglia, A. Casnati, L. Mandolini and R. Ungaro, *Chem.-Eur. J.*, 2000, **6**, 1322.
- H. C. Visser, D. N. Reinhoudt and F. Jong, *Chem. Soc. Rev.*, 1994, **94**, 75.
- F. J. B. Kremer, G. Chiosis, J. F. J. Engbersen and D. N. Reinhoudt, *J. Chem. Soc., Perkin Trans. 2*, 1994, 677.
- D. Diamond and M. A. McKervey, *Chem. Soc. Rev.*, 1996, **25**, 15.
- T. Ogoshi, S. Kanai, S. Fujinami, T. Yamagishi and Y. Nakamoto, *J. Am. Chem. Soc.*, 2008, **130**, 5022.
- T. Ogoshi, K. Umeda, T. Yamagishi and Y. Nakamoto, *Chem. Commun.*, 2009, 4874.
- T. Ogoshi, K. Kitajima, T. Yamagishi and Y. Nakamoto, *Org. Lett.*, 2010, **12**, 636.
- T. Ogoshi, M. Hashizume, T. Yamagishi and Y. Nakamoto, *Chem. Commun.*, 2010, **46**, 3708.
- T. Ogoshi, K. Kitajima, T. Aoki, S. Fujinami, T. Yamagishi and Y. Nakamoto, *J. Org. Chem.*, 2010, **75**, 3268.
- T. Ogoshi, T. Aoki, K. Kitajima, S. Fujinami, T. Yamagishi and Y. Nakamoto, *J. Org. Chem.*, 2011, **76**, 328.
- T. Ogoshi, K. Kitajima, T. Aoki, T. Yamagishi and Y. Nakamoto, *J. Phys. Chem. Lett.*, 2010, **1**, 817.
- C. Li, Q. Xu, J. Li, F. Yao and X. Jia, *Org. Biomol. Chem.*, 2010, **8**, 1568.
- T. Ogoshi, Y. Nishida, T. Yamagishi and Y. Nakamoto, *Macromolecules*, 2010, **43**, 3145.
- C. Li, L. Zhao, J. Li, X. Ding, S. Chen, Q. Zhang, Y. Yu and X. Jia, *Chem. Commun.*, 2010, **46**, 9016.
- T. Ogoshi, Y. Nishida, T. Yamagishi and Y. Nakamoto, *Macromolecules*, 2010, **43**, 7068.
- X. Hu, L. Chen, W. Si, Y. Yu and J. Hou, *Chem. Commun.*, 2011, **47**, 4694.
- T. Ogoshi, R. Shiga, T. Yamagishi and Y. Nakamoto, *J. Org. Chem.*, 2011, **76**, 618.
- W. Si, X. Hu, R. Fan, Z. Chen, L. Weng and J. Hou, *Tetrahedron Lett.*, 2011, **52**, 2484.
- Y. Kou, H. Tao, D. Cao, Z. Fu, D. Schollmeyer and H. Meier, *Eur. J. Org. Chem.*, 2010, 6464.
- Z. Zhang, Y. Luo, B. Xia, C. Han, Y. Yu, X. Chen and F. Huang, *Chem. Commun.*, 2011, **47**, 2417.
- B. Xia, J. He, Z. Abliz, Y. Yu and F. Huang, *Tetrahedron Lett.*, 2011, **52**, 4433.
- Z. Zhang, B. Xia, C. Han, Y. Yu and F. Huang, *Org. Lett.*, 2010, **12**, 3285.
- T. Ogoshi, R. Shiga, M. Hashizume and T. Yamagishi, *Chem. Commun.*, 2011, **47**, 6927.
- T. Ogoshi, K. Demachi, K. Kitajima and T. Yamagishi, *Chem. Commun.*, 2011, **47**, 7164.

- 44 N. L. Strutt, R. S. Forgan, J. M. Spruell, Y. Y. Botros and J. F. Stoddart, *J. Am. Chem. Soc.*, 2011, **133**, 5668.
- 45 T. Ogoshi, K. Masaki, R. Shiga, K. Kitajima and T. Yamagishi, *Org. Lett.*, 2011, **13**, 1264.
- 46 T. Ogoshi, *J. Inclusion Phenom. Macrocyclic Chem.*, 2012, **72**, 247.
- 47 P. J. Cragg and K. Sharma, *Chem. Soc. Rev.*, 2012, **41**, 597.
- 48 D. Cao, Y. Kou, J. Liang, Z. Chen, L. Wang and H. Meier, *Angew. Chem., Int. Ed.*, 2009, **48**, 9721.
- 49 C. Han, F. Ma, Z. Zhang, B. Xia, Y. Yu and F. Huang, *Org. Lett.*, 2010, **12**, 4360.
- 50 H. Tao, D. Cao, L. Liu, Y. Kou, L. Wang and H. Meier, *Sci. China: Chem.*, 2012, **55**, 223.
- 51 K.-U. Lao and C.-H. Yu, *J. Comput. Chem.*, 2011, **32**, 2716.
- 52 R. V. Pinjari, K. A. Joshi and S. P. Gejji, *J. Phys. Chem. A*, 2006, **110**, 13073.
- 53 R. V. Pinjari, K. A. Joshi and S. P. Gejji, *J. Phys. Chem. A*, 2007, **111**, 13583.
- 54 R. V. Pinjari and S. P. Gejji, *J. Phys. Chem. A*, 2008, **112**, 12679.
- 55 R. V. Pinjari, J. K. Khedkar and S. P. Gejji, *J. Inclusion Phenom. Macrocyclic Chem.*, 2010, **66**, 371.
- 56 V. V. Gobre, R. V. Pinjari and S. P. Gejji, *J. Phys. Chem. A*, 2010, **114**, 4464.
- 57 R. V. Pinjari and S. P. Gejji, *J. Phys. Chem. A*, 2010, **114**, 2338.
- 58 H. S. Frank and W. Y. Wen, *Discuss Faraday Soc.*, 1957, **24**, 133–140.
- 59 Huyskens, *J. Am. Chem. Soc.*, 1977, **99**, 2578.
- 60 A. D. Becke, *Phys. Rev. A*, 1988, **38**, 3098.
- 61 C. Lee, W. Yang and R. G. Parr, *Phys. Rev. B*, 1988, **37**, 785.
- 62 M. J. Frisch, G. W. Trucks, H. B. Schlegel, G. E. Scuseria, M. A. Robb, J. R. Cheeseman, G. Scalmani, V. Barone, B. Mennucci, G. A. Petersson, H. Nakatsuji, M. Caricato, X. Li, H. P. Hratchian, A. F. Izmaylov, J. Bloino, G. Zheng, J. L. Sonnenberg, M. Hada, M. Ehara, K. Toyota, R. Fukuda, J. Hasegawa, M. Ishida, T. Nakajima, Y. Honda, O. Kitao, H. Nakai, T. Vreven, J. A. Jr. Montgomery, J. E. Peralta, F. Ogliaro, M. Bearpark, J. J. Heyd, E. Brothers, K. N. Kudin, V. N. Staroverov, R. Kobayashi, J. Normand, K. Raghavachari, A. Rendell, J. C. Burant, S. S. Iyengar, J. Tomasi, M. Cossi, N. Rega, J. M. Millam, M. Klene, J. E. Knox, J. B. Cross, V. Bakken, C. Adamo, J. Jaramillo, R. Gomperts, R. E. Stratmann, O. Yazyev, A. J. Austin, R. Cammi, C. Pomelli, J. W. Ochterski, R. L. Martin, K. Morokuma, V. G. Zakrzewski, G. A. Voth, P. Salvador, J. J. Dannenberg, S. Dapprich, A. D. Daniels, O. Farkas, J. B. Foresman, J. V. Ortiz, J. Cioslowski and D. J. Fox, *Gaussian 09, Revision A.02*, Gaussian, Inc., Wallingford CT, 2009.
- 63 R. Bonaccorsi, E. Scrocco and J. Tomasi, *J. Chem. Phys.*, 1970, **52**, 5270.
- 64 R. Bonaccorsi, E. Scrocco and J. Tomasi, *Theor. Chim. Acta (Berlin)*, 1979, **52**, 113.
- 65 S. R. Gadre and I. H. Shrivastava, *J. Chem. Phys.*, 1991, **94**, 4384.
- 66 S. R. Gadre, C. Komel, M. Ehrig and R. Z. Ahlrichs, *Naturforscher*, 1993, **48a**, 145.
- 67 A. C. Limaye and S. R. Gadre, *Curr. Sci.*, 2001, **80**, 1298.
- 68 R. F. W. Bader, *Atoms in Molecules: A Quantum Theory*, Oxford University Press, Oxford, UK, 1990.
- 69 D. F. Matta and R. J. Boyd, *The Quantum theory of Atoms in Molecules*, in *An Introduction to the Quantum Theory of Atoms in Molecules*, ed. D. F. Matta and R. J. Boyd, Wiley-VCH, Weinheim, 2007, p. 1.
- 70 P. Popelier, *Molecular Similarity in Drug Design*, ed. P. M. Dean, Blackie (Glasgow), 1995, p. 215.
- 71 P. Balanarayan and S. R. Gadre, *J. Chem. Phys.*, 2003, **119**, 5037.
- 72 A. E. Reed, L. A. Curtiss and F. Weinhold, *Chem. Res.*, 1988, **88**, 899.
- 73 K. Wolinski, J. F. Hilton and P. Pulay, *J. Am. Chem. Soc.*, 1990, **112**, 8251.
- 74 S. Miertus, E. Scrocco and J. Tomasi, *J. Chem. Phys.*, 1981, **55**, 117.
- 75 V. V. Gobre, P. H. Dixit, J. K. Khedkar and S. P. Gejji, *Comput. Theor. Chem.*, 2011, **976**, 76.